BIOSYSTEMS ENGINEERING 223 (2022) 149–160

Available online at www.sciencedirect.com

ScienceDirect

journal homepage: www.elsevier.com/locate/issn/15375110

Research Paper

Verification and error analysis for the simulation of the grain mass aeration process using the method of manufactured solutions

Daniel Rigoni [a,*], *Marcio A.V. Pinto* [b], *Jotair E. Kwiatkowski Jr.* [c]

[a] *Graduate Program in Numerical Methods in Engineering, Federal University of Paraná, 81531-980, Curitiba, PR, Brazil*

[b] *Department of Mechanical Engineering, Federal University of Paraná, 81531-980, Curitiba, PR, Brazil*

[c] *Department of Computer Science, State University of Centro-Oeste, 85040-167, Guarapuava, PR, Brazil*

ARTICLE INFO

Article history:
Received 17 February 2022
Received in revised form
16 August 2022
Accepted 23 August 2022

Keywords:
Artificial viscosity
Grain storage
Thorpe model
Crank-Nicolson
Roberts and Weiss
Leith

The goal of this paper is to present an analytical solution, by means of the method of manufactured solutions (MMS), for the mathematical model that describes the behaviour of the grain mass aeration process, proposed by Thorpe. In contrast to related papers in the literature, several numerical approximations to solve the mathematical model were used. The finite difference method (FDM), employing the spatial approximations given by the methods of Roberts and Weiss, Leith, upwind difference scheme (UDS), central difference scheme (CDS) and UDS with deferred correction (UDS-C), combined with the explicit, implicit and Crank-Nicolson temporal formulations was applied. The effective order of the discretisation error achieved with the refinement of the mesh was verified by performing an error analysis for all approximations used. In addition, the results obtained numerically were compared to the analytical solution and the CPU (central processing unit) times at different levels of refinement. The difference in the CPU time using the methods CDS - Crank-Nicolson, Roberts and Weiss, and Leith, was very small compared to the method widely used in literature, the UDS - Explicit. It was also verified that the errors obtained by the proposed methods were considerably smaller than the error obtained by the UDS - Explicit method. In light of the above, the Leith method is recommended to numerically solve the grain mass aeration model proposed by Thorpe.

1. Introduction

The use of information and communication technology (ICT) across different sectors of the global economy has become essential to increase efficiency and productivity. One of the industries that has been highly impacted by the application of ICT across all spheres of its operation is the agricultural sector (Nyarko & Kozári, 2021). Daum (2019) observed that in recent years, ICT has become one of the main allies of farmers to manage essential factors of production in agriculture, such as grain storage.

* *Corresponding author.*
E-mail address: rigoni1@ufpr.br (D. Rigoni).

https://doi.org/10.1016/j.biosystemseng.2022.08.006

Nomenclature

Abbreviations

CDS	Central difference scheme
CPU	Central processing unit
FDM	Finite difference method
ICT	Information and communication technology
LS	Leith scheme
MMS	Method of manufactured solutions
PDE	Partial differential equation
RWS	Roberts and Weiss scheme
TDMA	Tri Diagonal matrix algorithm
UDS	Upwind difference scheme
UDS-C	UDS with deferred correction

Variables

A, B, C	Constants that vary according to the type of grain
β	Mixing factor between the UDS and CDS schemes
c_a	Specific heat of air ($Jkg^{-1}{}^{\circ}C^{-1}$)
c_g	Grain specific heat ($Jkg^{-1}{}^{\circ}C^{-1}$)
C_i	Coefficients
c_W	Specific heat of water ($Jkg^{-1}{}^{\circ}C^{-1}$)
D	Dimensionless constant
$\frac{dm}{dt}$	Derivative of the grain dry matter loss with respect to time (kgs^{-1})
Δt	Difference between the current simulation time and the previous one
Δy	Spacing between two consecutive nodes
E	Numerical error
ε	Grain porosity (decimal)
$erfc$	Complementary error function
h	Representative mesh size
h_s	Differential heat of sorption (Jkg^{-1})
h_v	Latent heat of vaporisation of water (Jkg^{-1})
M_T	Parameter used to adjust the aeration time according to the temperature
M_U	Parameter used to adjust the aeration time according to the water content
N	Number of unknowns
n	Temporal location of the node
N_t	Number of time steps
N_y	Number of nodes in the y direction
P	Central node
P_{atm}	Atmospheric pressure (Pa)
p_E	Effective order
p_L	Asymptotic order
p_s	Saturation vapour pressure (Pa)
q	Mesh refinement ratio
Q_r	Heat of oxidation of the grain ($Js^{-1}m^{-3}$)
R	Humidity ratio of air ($kgkg^{-1}$)
ρ_a	Density of intergranular air (kgm^{-3})
ρ_σ	Grain bulk density (kgm^{-3})
r_a	Relative humidity of the aeration air (%)
r_u	Equilibrium relative humidity (%)
S, $\mathcal{A}$, $\mathcal{B}$, $\mathcal{F}$	Parameters used to simplify notation
S_T	Source term
T	Grain temperature (°C)
t	Time (s)
θ	Represents the temporal formulation used
T_{amb}	Ambient temperature (°C)
$T_{An}(y)$	Represent the analytically obtained temperature (°C)
T_B	Aeration air temperature (°C)
t_f	Final simulation time (s)
T_I	Initial grain temperature (°C)
$T_{Num}(y)$	Represent the numerically obtained temperature (°C)
$T^*_{P,CDS}$, $T^*_{P,UDS}$	Known values from the previous iteration
U	Grain moisture ($kgkg^{-1}$)
u_a	Aeration air velocity (ms^{-1})
U_I	Initial grain moisture ($kgkg^{-1}$)
U_p	Initial grain moisture content in percent (%)
u_r	Ambient relative humidity (%)
W, E	Identifiers of the position of discrete points in relation to a central node
y	Axis in the vertical direction (oriented from bottom to top) (m)
$\|\|.\|\|_2$	Standard L_2-norm

Adequate grain storage is the main contributor to protecting the quality of the final product. According to Antunes et al. (2016), the most widespread control method employed in the preservation of stored grains is aeration, which consists of the forced passage of air through the stored grain mass. The aeration process reduces and stabilises the grain mass temperature in order to preserve the stored grains (Ziegler et al., 2021).

Despite the large scale of agricultural production and the use of techniques to improve the quality of grain mass, investments in technology are still modest, especially among small grain producers. In this sense, studies involving mathematical models and computational resolutions are relevant.

Mathematical models have been used to describe both theoretical and observed phenomena. In addition, they simulate and predict the outcome of various applications, regardless of the prevailing conditions. Moreover, the most promising results during simulation can be tested in the field (Nuttall et al., 2017). Several mathematical models can be found in the literature involving the aeration process, such as, Thompson et al. (1968), Sinicio et al. (1997), Jia et al. (2001), Thorpe (2001b) and Khatchatourian and Oliveira (2006).

In this paper, the model proposed by Thorpe (2001b), frequently found in the literature (Lopes et al., 2006, 2014, 2015; Rigoni & Kwiatkowski Jr., 2020), whose analytical solution is unknown, is applied. In these studies, the finite difference method (FDM), combined with the upwind difference scheme (UDS) spatial discretisation and the explicit temporal formulation was used to solve Thorpe's model numerically.

When a model is solved numerically, it is important to pursue efficient and accurate ways to solve problems. Thus, alternative methods with known efficiency that have not yet been applied to solve this particular problem, deserve attention. In this sense, the application to practical problems might

be of great contribution as models can be used to efficiently test different approaches, which can take years in the field and have significant cost (Nuttall et al., 2017).

The goal of this paper is to present an analytical solution for the Thorpe model, by means of the Method of Manufactured Solutions (MMS). The FDM was used to solve the model numerically and, unlike the previously cited papers, spatial approximations, given by the methods of Leith (1965), Roberts and Weiss (1966), UDS, CDS, and UDS-C, were employed, combined with the explicit, implicit and Crank-Nicolson temporal formulations.

Following a variety of examples found in the literature, including Xuan et al. (2017), Mousa and Ma (2020), and Melland et al. (2021), the technique presented by Von Neumann and Richtmyer (1950) was chosen to treat non-physical oscillations in the second-order approximations.

Besides proposing an analytical solution for the mathematical model and using different approximations than those already existing in the literature, the novelty of this paper includes performing an error analysis for all the approximations used to verify the effective order of the discretisation error with the refinement of the mesh. In addition, the CPU (central processing unit) times were compared with the results obtained numerically using the analytical solution at different levels of mesh refinement to determine which approximations perform more efficiently.

The remainder of this paper is organised as follows. In section 2, the mathematical model proposed by Thorpe (2001b) and the boundary and initial conditions are presented. In section 3, an analytical solution using the MMS is proposed. The numerical resolution of the mathematical model is shown in section 4. In section 5, the criteria used for the numerical verification are introduced. In section 6, the effective orders and discretisation errors for each approximation used and the results obtained are demonstrated, and, in section 7, conclusions are drawn.

2. Mathematical model

The model that describes the temperature (T) and the grain moisture (U) used in this work was presented in detail by Thorpe (2001b). According to Lopes et al. (2006), some simplifications can be made in the original model without losing accuracy. The simplified model, which was adopted in this paper, is given by

$$\frac{\partial T}{\partial t}\left\{\rho_\sigma\left[c_g + c_W U\right] + \varepsilon\rho_a\left[c_a + R\left(c_W + \frac{\partial h_v}{\partial T}\right)\right]\right\} = \rho_\sigma h_s \frac{\partial U}{\partial t} - u_a\rho_a \left[c_a + R\left(c_W + \frac{\partial h_v}{\partial T}\right)\right]\frac{\partial T}{\partial y} + \rho_\sigma \frac{dm}{dt}\left(Q_r - 0.6h_v\right) \quad (1)$$

$$\rho_\sigma \frac{\partial U}{\partial t} = -u_a\rho_a\frac{\partial R}{\partial y} + \frac{dm}{dt}(0.6 + U) \quad (2)$$

where: t is time (s), y is the axis in the vertical direction (oriented from bottom to top) (m), U is grain moisture (kgkg^{-1}), u_a is aeration air velocity (ms^{-1}), c_g is grain specific heat (Jkg^{-1}°C^{-1}), c_W is specific heat of water (Jkg^{-1}°C^{-1}), c_a is specific heat of air (Jkg^{-1}°C^{-1}), R is humidity ratio of air (kgkg^{-1}), ρ_a is density of intergranular air (kgm^{-3}), ρ_σ is grain bulk density (kgm^{-3}), h_v is latent heat of vaporisation of water (Jkg^{-1}), h_s is differential heat of sorption (Jkg^{-1}), T is grain temperature (°C), ε is grain porosity (decimal), $\frac{dm}{dt}$ is derivative of the grain dry matter loss with respect to time (kgs^{-1}) and Q_r is heat of oxidation of the grain (Js^{-1}m^{-3}).

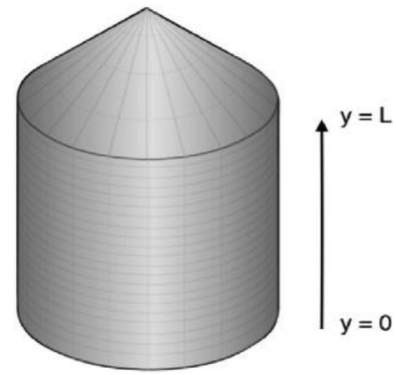

Fig. 1 – Calculation domain.

An up-flow aeration system was considered, that is $y \in [0, L]$, where L represents the height of the grain mass, as shown in Fig. 1. Therefore, a one-dimensional simplification of the model was considered.

Although this paper deals with a simplified one-dimensional model of the problem, Fig. 1 shows a realistic three-dimensional silo for better visualisation of the geometry in which the numerical analysis is performed.

The aeration air velocity (u_a) is the velocity at which the air flows through the stored grain mass. According to Brooker et al. (1992), the specific heat of water (c_W) and the specific heat of air (c_a) are well-defined quantities, equal to 4186 (Jkg^{-1}°C^{-1}) and 1000 (Jkg^{-1}°C^{-1}), respectively.

In this paper, data obtained by Brooker et al. (1992) for grain porosity ($\varepsilon = 0.361$) was used, which can be defined as the ratio between the volume occupied by the air in the grain mass and the total volume occupied by this mass, and greatly influences the pressure of airflows passing through the grain mass.

The grain bulk density ρ_σ determines the volume required to store a given quantity of a product and directly influences the airflow rate required for aeration and the heat and mass transfer process in the storage environment (Lopes et al., 2006). The value of the grain bulk density ($\rho_\sigma = 737$ kgm^{-3}) was considered following the data shown by Thorpe (2001a).

According to Fleurat-Lessard (2002), the heat of oxidation of the grain (Q_r) is equal to 15,778 (Js^{-1}m^{-3}). The grain specific heat (c_g) also affects the heat and mass transfer process during aeration (Navarro & Noyes, 2001), and as stated by Lopes et al. (2006), it represents the amount of thermal energy required to increase the temperature of 1 kg of a product by 1 °C. Data from Jayas & Cenkowski (2006) was used to determine the grain specific heat ($c_g = 1637$ Jkg^{-1}°C^{-1}).

The differential heat of sorption (h_s), as well as the latent heat of vaporisation of water (h_v), are key properties considered in the simulation of the aeration process, as they interfere with the heat and mass transfer inside the storage environment (Lopes et al., 2006). According to Thorpe (2001b),

h_s is the total energy required to remove one unit mass of water from the grain mass and is given by

$$h_s = h_v\left[1 + \frac{Ae^{-BU}(T+273.15)}{(T+C)^2 - 5 + \frac{6800}{T+273.15}}\right] \tag{3}$$

A, B e C are constants that vary according to the type of grain, as detailed by Pfost et al. (1976).

As stated by Thorpe (2001b), the heat applied to water that causes it to change from liquid to vapor is called the latent heat of vaporisation of water (h_v) and can be calculated by

$$h_v = 2501.33 - 2.363T \tag{4}$$

In order to correct possible altitude effects, the density of intergranular air (ρ_a) can be calculated, as (Lopes et al., 2006):

$$\rho_a = \frac{258.8P_{atm}}{101.325(T+273.15)} \tag{5}$$

where P_{atm} is the atmospheric pressure.

With respect to time, the derivative of the grain dry matter loss ($\frac{dm}{dt}$) can be estimated via models obtained by fitting mathematical relationships to experimental data. In this work, the model presented by Thompson (1972) was employed:

$$\frac{dm}{dt} = 8.83\times10^{-4}\left\{exp\left[1.667\times10^{-6}\frac{t}{M_U M_T}\right] - 1\right\} + 2.833 \times10^{-9}\frac{t}{M_U M_T} \tag{6}$$

where M_U and M_T are parameters used to adjust the aeration time according to the water content and temperature of the grains. The parameter M_U can be obtained by

$$M_U = 0.103\left(exp\left[\frac{455}{(100U)^{1.53}}\right] - 0.845U + 1.558\right) \tag{7}$$

and M_T can be obtained according to the temperature and moisture range:

$$\begin{cases} M_T = S, \text{if } T \le 15 \text{ or } U \le 19 & (8a)\\ M_T = S + \frac{\frac{100U}{U+1} - 19}{100}\, exp[0.0183T - 0.2847], \text{if } T > 15 \text{ and } 19 < U < 28 & (8b)\\ M_T = S + 0.09\, exp[0.0183T - 0.2847], \text{if } T > 15 \text{ and } U \ge 28 & (8c)\end{cases}$$

where $S = 32.2\, exp(-0.1044T - 1.856)$.

The humidity ratio of air (R) is the ratio between the mass of water vapor and the mass of dry air in a given mixing volume. This parameter was used to model the behaviour of the grain mass during the aeration process, contributing to estimating the water content of the stored product and assisting in predicting the effects of aeration in the storage environment. It can be calculated as (Thorpe, 2001a):

$$R = 0.622\frac{r_u p_s}{P_{atm} - r_u p_s} \tag{9}$$

where p_s is the saturation vapor pressure given as (Hunter, 1987):

$$p_s = \frac{6\times10^{25}}{(T+273.15)^5}exp\left[-\frac{6800}{T+273.15}\right] \tag{10}$$

and r_u represents the equilibrium relative humidity and can be calculated as (Chung & Pfost, 1967):

$$r_u = 100\, exp\left[-\frac{A}{T+C}exp(-BU)\right] \tag{11}$$

2.1. Boundary conditions

At y = 0, it was assumed that the grains at the base of the storage come to equilibrium with the aeration airflow:

$$T(0,t) = T_B \tag{12}$$

where T_B represents the aeration air temperature.

The moisture at y = 0 was calculated as:

$$U(0,t) = -\frac{1}{B}ln\left[ln\left(-\frac{r_a}{100}\right)\left(-\frac{T_B + C}{A}\right)\right] = U_B \tag{13}$$

which is an adaptation of the Chung-Pfost equation (Eq. (11)) where r_a represents the relative humidity of the aeration airflow and can be obtained by

$$r_a = u_r\frac{\frac{6\times10^{25}}{(T_{amb}+273.15)^5}exp\left[-\frac{6800}{T_{amb}+273.15}\right]}{\frac{6\times10^{25}}{(T_B+273.15)^5}exp\left[-\frac{6800}{T_B+273.15}\right]} \tag{14}$$

where u_r is the ambient relative humidity and T_{amb} is the ambient temperature.

At y = L, Neumann boundary conditions for the temperature and moisture were given by

$$\left(\frac{\partial T}{\partial y}\right)_{y=L} = \left(\frac{\partial U}{\partial y}\right)_{y=L} = 0 \tag{15}$$

2.2. Initial conditions

Throughout the domain, the initial condition was equal to the grain bulk temperature after the drying process (T_I).

$$T(y,0) = T_I \tag{16}$$

The initial moisture (U_I) can be obtained as (Thorpe, 2001b)

$$U(y,0) = \frac{U_p}{100 - U_p} = U_I \tag{17}$$

where U_p is the grain moisture content after drying, in percentage (%).

3. Method of manufactured solutions (MMS)

The method of manufactured solutions (MMS) (Oberkampf & Blottner, 1998) consists of producing an exact solution with no interest in the physical reality of the problem. An analytic function is defined and used as the dependent variable in the partial differential equation (PDE), and all derivatives are calculated analytically. The equation is created in a way that all remaining terms that do not satisfy the PDE are incorporated into a source term. This term is then added to the PDE to exactly satisfy the new PDE (Roy, 2005).

Despite the many uses of the model proposed by Thorpe (2001b) found in the literature, hereinafter referred to as Thorpe model, there is no investigation of the analytical solution of the mathematical model. In order to find an analytical solution for the temperature (Eq. (1)), experimental data presented by Khatchatourian and Oliveira (2006) and Oliveira et al. (2007) was considered as baseline. The experiment measured the temperature of soybeans in a prototype silo measuring one metre of height ($L = 1$ m), with thermocouples at 0.15 m, 0.27 m, 0.40 m, and 0.54 m height, during 1 h of aeration. At the beginning of the experiment, the grain temperature was $T_I = 52.9$ °C and the aeration air temperature was $T_B = 31.1$ °C.

The analytical solution for Eq. (1) proposed in this paper was fabricated based on modifying a solution of a problem presented by Van Genuchten et al. (1982), and it is given by

$$\begin{aligned}\widehat{T}(y,t) \quad &= T_I + \frac{1}{2}(T_B - T_I)\left[erfc\left(\frac{y - 2.2\times10^{-4}t}{\sqrt{8\times10^{-6}t}}\right)\right.\\ &\left.+exp\left(\frac{2.2\times10^{-4}y}{8\times10^{-6}}\right)erfc\left(\frac{y + 2.2\times10^{-4}t}{\sqrt{8\times10^{-6}t}}\right)\right]\end{aligned} \tag{18}$$

where *erfc* represents the complementary error function (Van Genuchten et al., 1982), defined by

$$erfc(x) = 1 - erf(x) = \frac{2}{\sqrt{\pi}}\int_x^\infty e^{-t^2}dt \tag{19}$$

The solution given by Eq. (18) was fabricated to satisfy an experiment performed on soybeans by Khatchatourian and Oliveira (2006) and Oliveira et al. (2007), well mentioned in the literature. The solution took as parameters the size of the storage (y), the aeration time (t), the temperature of the aeration air (T_B), and the grain mass initial temperature (T_I).

The solution proposed in this paper, given by Eq. (18), tends to satisfy the conditions of real aeration systems, which can take between 300 and 600 h to complete, have different geometries, different grain initial temperatures, and different aeration air temperatures, with minor modifications. Regarding different types of grain, more elaborate modifications are required and such adaptations should be further investigated.

For the function defined by Eq. (18) to be considered an analytical solution of Eq. (1), a source term (S_T) must be added to the governing equation:

$$\frac{\partial T}{\partial t}\left\{\rho_\sigma\left[c_g + c_W U\right] + \varepsilon\rho_a\left[c_a + R\left(c_W + \frac{\partial h_v}{\partial T}\right)\right]\right\} =$$

$$\rho_\sigma h_s\frac{\partial U}{\partial t} - u_a\rho_a\left[c_a + R\left(c_W + \frac{\partial h_v}{\partial T}\right)\right]\frac{\partial T}{\partial y} + \rho_\sigma\frac{dm}{dt}(Q_r - 0.6h_v) + S_T \tag{20}$$

where S_T is given by

$$S_T = \frac{\partial\widehat{T}}{\partial t}\left\{\rho_\sigma\left[c_g + c_W U\right] + \varepsilon\rho_a\left[c_a + R\left(c_W + \frac{\partial h_v}{\partial T}\right)\right]\right\}$$

$$-\rho_\sigma h_s\frac{\partial U}{\partial t} + u_a\rho_a\left[c_a + R\left(c_W + \frac{\partial h_v}{\partial T}\right)\right]\frac{\partial\widehat{T}}{\partial y} - \rho_\sigma\frac{dm}{dt}(Q_r - 0.6h_v) \tag{21}$$

Furthermore, $\frac{\partial\widehat{T}}{\partial t}$ and $\frac{\partial\widehat{T}}{\partial y}$ must be calculated, substituting Eq. (21) into Eq. (20), making some simplifications and denoting $\mathcal{A}$, $\mathcal{B}$ and $\mathcal{F}$, as

$$\mathcal{A} = \rho_\sigma\left[c_g + c_W U\right] + \varepsilon\rho_a\left[c_a + R\left(c_W + \frac{\partial h_v}{\partial T}\right)\right] \tag{22}$$

$$\mathcal{B} = u_a\rho_a\left[c_a + R\left(c_W + \frac{\partial h_v}{\partial T}\right)\right] \tag{23}$$

$$\mathcal{F} = \mathcal{A}\left(\frac{1}{2}(T_B - T_I)\left[-\frac{2\,exp\left[\frac{-125000\left(y-2.2\times10^4 t\right)^2}{t}\right]\left(-\frac{176.777\left(y-2.2\times10^{-4}t\right)}{t^{\frac{3}{2}}}-\frac{0.0777817}{\sqrt{t}}\right)}{\sqrt{\pi}}-\frac{2\,exp\left[27.5y-\frac{125000\left(2.2\times10^4 t+y\right)^2}{t}\right]\left(\frac{0.0777817}{\sqrt{t}}-\frac{176.777\left(2.2\times10^{-4}t+y\right)}{t^{\frac{3}{2}}}\right)}{\sqrt{\pi}}\right]\right)$$
$$+\mathcal{B}\left(\frac{1}{2}(T_B - T_I)\times\left[27.5\,exp(27.5y)erfc\left(\frac{353.553\left(2.2\times10^{-4}t+y\right)}{\sqrt{t}}\right)-\frac{398.942\,exp\left[\frac{-125000\left(y-2.2\times10^{-4}t\right)^2}{t}\right]}{\sqrt{t}}-\frac{398.942\,exp\left[27.5y-\frac{125000\left(2.2\times10^{-4}t+y\right)^2}{t}\right]}{\sqrt{t}}\right]\right) \quad (24)$$

the equation that describes the temperature (T) of the grain mass is presented as follows:

$$\mathcal{A}\frac{\partial T}{\partial t} = -\mathcal{B}\frac{\partial T}{\partial y} + \mathcal{F} \quad (25)$$

whose analytical solution is given by Eq. (18) through the MMS.

It is important to highlight that in this paper, the MMS was used to compare several discretisation schemes. It was also assumed that an equation that captures advection and dispersion in porous media provides an adequate analytical solution. Such an equation was compared with experimental data on the cooling of soybeans. Eqs. (1) and (2) do not contain terms that account for the dispersion, and the spreading of the waves arises from soybean properties. These facts do not detract from the analysis because the method of manufactured solutions does not rely on an accurate representation of reality.

4. Numerical model

The differential equations that describe the grain temperature and moisture were solved numerically by means of the finite difference method (FDM) (Tannehill et al., 1997).

After a given equation is discretised using the FDM, the evaluation of the variables and the approximations of their derivatives at the mesh nodes originate a system of equations that must then be solved by an appropriate method, commonly called *solver*.

In this study, a *solver* extensively adopted in the literature called Tri Diagonal matrix algorithm (TDMA) (Thomas, 1949) was used for all approximations. For problems involving larger dimensions, or even slow convergence, other numerical techniques can be applied (Oliveira et al., 2018). W and E were used to identify the position of the discrete points in relation to a central node P and n, the temporal location of the node, as indicated in Fig. 2.

In Fig. 2, $\Delta y = \frac{L}{N_y}$ corresponds to the spacing between two consecutive nodes, where N_y is the number of nodes in the y direction; and $\Delta t = \frac{t_f}{N_t}$, the difference between the current simulation time and the previous one, where t_f is the final simulation time and N_t corresponds to the number of time steps.

4.1. *Upwind difference scheme (UDS)*

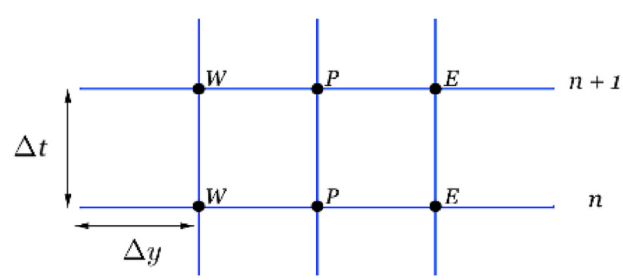

Fig. 2 – Mesh of the numerical solution using the FDM, for central node P, and its spatial and temporal neighbours.

By approximating the spatial derivative of T by means of UDS and the temporal derivative of T using the θ formulation, the discretised form of Eq. (25) is achieved:

$$\mathcal{A}^\theta T_P^{n+1} = \mathcal{A}^\theta T_P^n - \mathcal{B}^\theta\left(\frac{\Delta t}{\Delta y}\right)T_P^\theta + \mathcal{B}^\theta\left(\frac{\Delta t}{\Delta y}\right)T_W^\theta + \mathcal{F}\Delta t \quad (26)$$

where

$$\mathcal{A}^\theta = \rho_\sigma\left[c_g + c_W U_P^\theta\right] + \varepsilon\rho_a\left[c_a + R_P^\theta\left(c_W + \frac{\partial h_v}{\partial T}\right)\right] \quad (27)$$

$$\mathcal{B}^\theta = u_a\rho_a\left[c_a + R_P^\theta\left(c_W + \frac{\partial h_v}{\partial T}\right)\right] \quad (28)$$

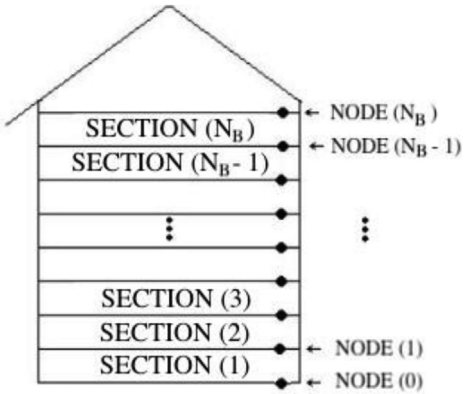

Fig. 3 – Discretised domain.

Using the same approximations for R, the discretised form of Eq. (2) is obtained:

$$U_P^{n+1} = U_P^n - \frac{u_a\rho_a}{\rho_\sigma}\left(\frac{\Delta t}{\Delta y}\right)R_P^\theta + \frac{u_a\rho_a}{\rho_\sigma}\left(\frac{\Delta t}{\Delta y}\right)R_W^\theta + \frac{\Delta t\frac{dm}{dt}}{\rho_\sigma}U_P^\theta + \frac{0.6\Delta t\frac{dm}{dt}}{\rho_\sigma} \tag{29}$$

in which the relation for an arbitrary variable Λ is given by

$$\Lambda^\theta = \Lambda^n + \theta\left(\Lambda^{n+1} - \Lambda^n\right) \tag{30}$$

where, if $\theta = 0$, there is an explicit formulation, if $\theta = 1$, there is an implicit formulation and if $\theta = 0.5$, there is the Crank-Nicolson formulation (Tannehill et al., 1997).

The Neumann boundary conditions can be approximated using UDS, thus the temperature and moisture at $y = L$ can be calculated, respectively, by

$$T_{N_B}^{n+1} = T_{N_B-1}^{n+1} \tag{31}$$

$$U_{N_B}^{n+1} = U_{N_B-1}^{n+1} \tag{32}$$

where N_B represents the node located at the boundary, as shown in Fig. 3.

4.2. Central difference scheme (CDS)

By approximating the spatial derivative of T utilising CDS and the temporal derivative of T using the θ formulation, the discretised form of Eq. (25) is given as:

$$\mathcal{A}^\theta T_P^{n+1} = \mathcal{A}^\theta T_P^n - \frac{\mathcal{B}^\theta}{2}\left(\frac{\Delta t}{\Delta y}\right)T_E^\theta + \frac{\mathcal{B}^\theta}{2}\left(\frac{\Delta t}{\Delta y}\right)T_W^\theta + \mathcal{F}\Delta t \tag{33}$$

where $\mathcal{A}^\theta$ and $\mathcal{B}^\theta$ are defined in the same form as Eqs. (27) and (28), respectively.

Using the same approximations for R, the discretised form of Eq. (2) is reached:

$$U_P^{n+1} = U_P^n - \frac{u_a\rho_a}{2\rho_\sigma}\left(\frac{\Delta t}{\Delta y}\right)R_E^\theta + \frac{u_a\rho_a}{2\rho_\sigma}\left(\frac{\Delta t}{\Delta y}\right)R_W^\theta + \frac{\Delta t\frac{dm}{dt}}{\rho_\sigma}U_P^\theta + 0.6\frac{\Delta t\frac{dm}{dt}}{\rho_\sigma} \tag{34}$$

The Neumann boundary conditions can be approximated using CDS combined with the ghost point technique (Tannehill et al., 1997), thus the temperature T and the moisture U at $y = L$ can be calculated, respectively, by

$$T_{N_B}^{n+1} = T_{N_B}^n + \mathcal{F}\frac{\Delta t}{\mathcal{A}} \tag{35}$$

$$U_{N_B}^{n+1} = U_{N_B}^n + \frac{\Delta t\frac{dm}{dt}}{\rho_\sigma}U_P^\theta + 0.6\frac{\Delta t\frac{dm}{dt}}{\rho_\sigma} \tag{36}$$

4.3. UDS with deferred correction (UDS-C)

Another approximation technique consists in mixing the UDS and CDS approximations, which results in the UDS with deferred correction, as follows:

$$T_P = T_{P,UDS} + \beta\left(T_{P,CDS}^* - T_{P,UDS}^*\right) \tag{37}$$

where $T_{P,CDS}^*$ and $T_{P,UDS}^*$ are known values from the previous iteration and are applied according to the scheme given by

$$\begin{cases} 0, \text{UDS} \\ \beta = 1, \text{CDS} \\ 0 < \beta < 1 \text{ Mixture} \end{cases} \tag{38}$$

By approximating the spatial derivative of T using UDS-C and the temporal derivative of T using the θ formulation, the discretised form of Eq. (25) is achieved:

$$\begin{aligned} \mathcal{A}^\theta T_P^{n+1} &= \mathcal{A}^\theta T_P^n - \mathcal{B}^\theta\left(\frac{\Delta t}{\Delta y}\right)T_P^\theta + \mathcal{B}^\theta\left(\frac{\Delta t}{\Delta y}\right)T_W^\theta \\ &\quad - \frac{\mathcal{B}^\theta\beta}{2}\left(\frac{\Delta t}{\Delta y}\right)\left[T_W^* - 2T_P^* + T_E^*\right] + \mathcal{F}\Delta t \end{aligned} \tag{39}$$

where $\mathcal{A}^\theta$ and $\mathcal{B}^\theta$ are defined in the same form as Eqs. (27) and (28), respectively.

Using the same approximations for R, the discretised form of Eq. (2) is reached:

$$\begin{aligned} U_P^{n+1} &= U_P^n - \frac{u_a\rho_a}{\rho_\sigma}\left(\frac{\Delta t}{\Delta y}\right)R_P^\theta + \frac{u_a\rho_a}{\rho_\sigma}\left(\frac{\Delta t}{\Delta y}\right)R_W^\theta \\ &\quad - \frac{u_a\rho_a\beta}{2\rho_\sigma}\left(\frac{\Delta t}{\Delta y}\right)\left[R_W^* - 2R_P^* + R_E^*\right] \\ &\quad + \frac{\Delta t\frac{dm}{dt}}{\rho_\sigma}U_P^\theta + \frac{0.6\Delta t\frac{dm}{dt}}{\rho_\sigma} \end{aligned} \tag{40}$$

The Neumann boundary conditions can be approximated using Eqs. (31) and (32).

4.4. Roberts and Weiss scheme (RWS)

According to Dehghan (2005) and Campbell & Yin (2007) the scheme proposed by Roberts & Weiss (1966) (RWS) consists in approximating the temporal and spatial derivatives of a variable Λ as follows:

$$\left(\frac{\partial\Lambda}{\partial t}\right)_P^{n+1} \approx \left[\frac{\Lambda_P^{n+1} - \Lambda_P^n}{\Delta t}\right] \tag{41}$$

$$\left(\frac{\partial\Lambda}{\partial y}\right)_P^{n+1} \approx \frac{1}{2}\left[\frac{\Lambda_P^{n+1} - \Lambda_W^{n+1}}{\Delta y} + \frac{\Lambda_E^n - \Lambda_P^n}{\Delta y}\right] \tag{42}$$

Thus, by approximating the spatial derivative of T using Eq.

(42) and the temporal derivative of T using Eq. (41), the discretised form of Eq. (25) is given as:

$$\left[2\mathcal{A}^{\theta}+\frac{\mathcal{B}^{\theta}\Delta t}{\Delta y}\right]T_P^{n+1}=\left[2\mathcal{A}^{\theta}+\frac{\mathcal{B}^{\theta}\Delta t}{\Delta y}\right]T_P^{n}+\left(\frac{\mathcal{B}^{\theta}\Delta t}{\Delta y}\right)T_W^{n+1}-\left(\frac{\mathcal{B}^{\theta}\Delta t}{\Delta y}\right)T_E^{n}+2\mathcal{F}\Delta t \tag{43}$$

where $\mathcal{A}^{\theta}$ and $\mathcal{B}^{\theta}$ are defined in the same way as in Eqs. (27) and (28), using $\theta = 0.5$.

Using the same approximations for R, the discretised form of Eq. (2) appears as:

$$U_P^{n+1}=\left[\frac{2\rho_\sigma}{2\rho_\sigma-\Delta t\frac{dm}{dt}}\right]\left[\left(1+\frac{\Delta t\frac{dm}{dt}}{2\rho_\sigma}\right)U_P^{n}-\frac{u_a\rho_a}{2\rho_\sigma}\left(\frac{\Delta t}{\Delta y}\right)\left(R_P^{n+1}-R_W^{n+1}+R_E^{n}-R_P^{n}\right)+\frac{0.6\Delta t\frac{dm}{dt}}{\rho_\sigma}\right] \tag{44}$$

The Neumann boundary conditions can be approximated using the ghost point technique (Tannehill et al., 1997), and the results are analogous to Eqs. (35) and (36).

4.5. Leith scheme (LS)

Eq. (25) can be rewritten as

$$\frac{\partial T}{\partial t}=-\left(\frac{\mathcal{B}}{\mathcal{A}}\right)\frac{\partial T}{\partial y}+\frac{\mathcal{F}}{\mathcal{A}} \tag{45}$$

The Leith Scheme (Leith, 1965) consists of approximating the temporal and space derivatives of T as follows:

$$\left(\frac{\partial T}{\partial t}\right)_P^{n+1}\approx\left[\frac{T_P^{n+1}-T_P^{n}}{\Delta t}\right] \tag{46}$$

$$\left(\frac{\partial T}{\partial y}\right)_P^{n+1}\approx\left(\frac{\mathcal{B}}{\mathcal{A}}\right)\left(\frac{\Delta t}{\Delta y}\right)\left[\frac{T_P^{n}-T_W^{n}}{\Delta y}\right]+\left[1-\left(\frac{\mathcal{B}}{\mathcal{A}}\right)\left(\frac{\Delta t}{\Delta y}\right)\right]\left[\frac{T_E^{n}-T_W^{n}}{2\Delta y}\right] \tag{47}$$

Thus, the discretised form of Eq. (45) is reached:

$$T_P^{n+1}=\left[1-\left(\frac{\mathcal{B}}{\mathcal{A}}\frac{\Delta t}{\Delta y}\right)^2\right]T_P^{n}+\frac{1}{2}\left[\left(\frac{\mathcal{B}}{\mathcal{A}}\frac{\Delta t}{\Delta y}\right)^2+\left(\frac{\mathcal{B}}{\mathcal{A}}\frac{\Delta t}{\Delta y}\right)\right]T_W^{n}+\frac{1}{2}\left[\left(\frac{\mathcal{B}}{\mathcal{A}}\frac{\Delta t}{\Delta y}\right)^2-\left(\frac{\mathcal{B}}{\mathcal{A}}\frac{\Delta t}{\Delta y}\right)\right]T_E^{n}+\mathcal{F}\frac{\Delta t}{\mathcal{A}} \tag{48}$$

The same procedure can be done on Eq. (2), resulting in the discretised form, given by

$$U_P^{n+1}=\left[\frac{2\rho_\sigma}{2\rho_\sigma-\frac{dm}{dt}\Delta t}\right]\left[\left(1+\frac{\frac{dm}{dt}\Delta t}{2\rho_\sigma}\right)U_P^{n}-\left(\frac{u_a\rho_a}{\rho_\sigma}\frac{\Delta t}{\Delta y}\right)^2R_P^{n}+\frac{1}{2}\left[\left(\frac{u_a\rho_a}{\rho_\sigma}\frac{\Delta t}{\Delta y}\right)^2+\left(\frac{u_a\rho_a}{\rho_\sigma}\frac{\Delta t}{\Delta y}\right)\right]R_W^{n}+\frac{1}{2}\left[\left(\frac{u_a\rho_a}{\rho_\sigma}\frac{\Delta t}{\Delta y}\right)^2-\left(\frac{u_a\rho_a}{\rho_\sigma}\frac{\Delta t}{\Delta y}\right)\right]R_E^{n}+\frac{0.6\Delta t\frac{dm}{dt}}{\rho_\sigma}\right] \tag{49}$$

The Neumann boundary conditions can be approximated using the ghost point technique (Tannehill et al., 1997), and the results are analogous to Eqs. (35) and (36).

4.6. Artificial viscosity

Formerly proposed by Von Neumann and Richtmyer (1950), artificial viscosity is a method to control non-physical spurious oscillations in numerical solutions and it can be added to the temperature equation. Thus, Eq. (25) can be rewritten as

$$\mathcal{A}\frac{\partial T}{\partial t}=-\mathcal{B}\frac{\partial T}{\partial y}+\frac{\partial}{\partial y}\left[D\Delta y^2\left|\frac{\partial T}{\partial y}\right|\frac{\partial T}{\partial y}\right]+\mathcal{F} \tag{50}$$

where D is a dimensionless constant (Campbell & Vignjevic, 2009). Noting that as $\Delta y \to 0$the term corresponding to the artificial viscosity tends to zero. Therefore, Eq. (50) tends to Eq. (25).

The method presented by Lax and Wendroff (1960) was used to perform the discretisation. For the problem in this study, artificial viscosity was used to eliminate excessive oscillations in the second-order methods. In this sense, it is adequate to add the following term in the discretised equations of these methods:

$$\frac{\partial}{\partial y}\left[D\Delta y^2\left|\frac{\partial T}{\partial y}\right|\frac{\partial T}{\partial y}\right]\approx\frac{D}{\Delta y}\left[\left|T_E^{n}-T_P^{n}\right|\left(T_E^{n}-T_P^{n}\right)-\left|T_P^{n}-T_W^{n}\right|\left(T_P^{n}-T_W^{n}\right)\right] \tag{51}$$

4.7. Computational details

The numerical resolutions were obtained using codes written in Fortran 95, using the Microsoft Visual Studio Code v. 1.62.0 with quadruple precision, and were compiled on a computer with a 3.4 GHz Intel Core i5 Quad-Core processor with 8 GB DDR3 RAM and an AMD Radeon 7850 2 GB graphic card. Simulations were performed varying the number of nodes and time steps for each method used.

Comparisons of the performances of the methods after the refinement of the mesh with the analytical solution, and during 1 h of aeration ($t_f = 3600$ s), were performed. To calculate the error between the numerical simulations and the proposed analytical solution, the L_2 - norm was used, defined by

$$L_2=\sum_{n=1}^{t_f}\left\|\,T_{Num}^{n}(y)-T_{An}^{n}(y)\,\right|_2 \tag{52}$$

where $\|.\|_2$ represents the standard L_2 - norm, $T_{Num}(y)$ and $T_{An}(y)$ represent the numerically and analytically obtained temperatures, respectively.

5. Error analysis

One of the novelties of this work consists in presenting an error analysis for all the approximations used. According to Marchi et al. (2016), the numerical error $E(\varphi)$ on a given variable of interest is defined as the difference between the analytical solution (Φ) and the numerical solution (φ):

$$E(\varphi)=\Phi-\varphi \tag{53}$$

where $E(\varphi)$ can appear in four forms (Marchi et al., 2016): truncation, iteration, rounding, and programming. When the other sources can be neglected, the truncation error (herein called discretisation error) $E(\varphi)$ is given, according to Roache (1998), by

$$E(\varphi) = C_1 h^{p_1} + C_2 h^{p_2} + C_3 h^{p_3} + \ldots \tag{54}$$

where h is the representative mesh size, C_i, $i = 1, 2, 3, \ldots$, are coefficients that are independent of h, but depend on the variable in question, and p_i, with $p_1 < p_2 < p_3 < \ldots$, are positive integers called true orders of the error. The first true order is called the asymptotic order and is denoted by $p_L = p_1$. The asymptotic order is a theoretical result obtained from the types of approximations used to discretise the problem.

The developed numerical model can be used to verify if the asymptotic order of the discretisation error is obtained. If the analytical solution to the problem is available, the effective order (p_E) of the discretization error can be used to estimate the asymptotic order. The effective order can be calculated as (Marchi et al., 2016)

$$p_E = \frac{\log\left(\frac{\Phi - \varphi_2}{\Phi - \varphi_1}\right)}{\log(q)} \tag{55}$$

where Φ is the exact analytical solution, φ_1 and φ_2, h_1 and h_2, are the numerical solutions and the representative sizes of the fine and coarse meshes, respectively, and $q = \frac{h_2}{h_1}$is the mesh refinement ratio. Theoretically, the effective order tends to the asymptotic order with mesh refinement, that is, $p_E \rightarrow p_L$ when $h \rightarrow 0$(Marchi et al., 2016). Table 1 shows the asymptotic order of each method used (Campbell & Yin, 2007; Dehghan, 2005; Tannehill et al., 1997).

According to Dehghan (2005), regarding the spatial approximation, the combination of CDS with the explicit temporal formulation is unstable for this type of problem and has no practical use. Thus, the methods CDS – Explicit and UDS-C – Explicit (combination of UDS – Explicit and CDS – Explicit) were not used.

6. Results and discussion

The results of this paper are presented in three subsections. In subsection 6.1, the analytical solution, proposed in this paper, is compared with experimental data. In subsection 6.2, the numerical verification is carried out, and in subsection 6.3, the performances of the methods are compared.

Table 1 – Asymptotic order of each method used (Campbell & Yin, 2007; Dehghan, 2005; Tannehill et al., 1997).

Method	Asymptotic Order (p_L)
UDS (Explicit; Implicit; Crank-Nicolson)	1
CDS (Explicit; Implicit)	1
UDS-C [β = 0.5] (Explicit; Implicit; Crank-Nicolson)	1
CDS (Crank-Nicolson), RWS and LS	2

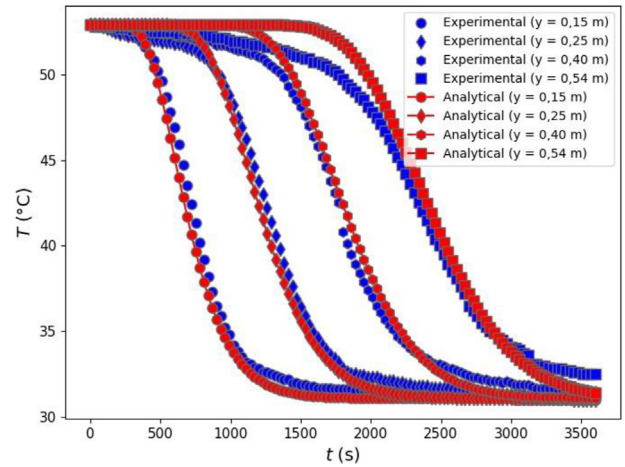

Fig. 4 – Analytical solution proposed in this paper and the experimental data (Khatchatourian & Oliveira, 2006; Oliveira et al., 2007).

6.1. Analytical solution and experimental data

Figure 4 shows Eq. (18) applied to the same points as the experimental data (Khatchatourian & Oliveira, 2006; Oliveira et al., 2007), using $T_I = 52.9$ °C and $T_B = 31.1$ °C.

It is possible to notice that the analytical solution (in red) presented a behaviour similar to that of the experimental data (in blue). Moreover, when the grain temperature started to drop (approximately after 450 s for the layer at y = 0.15 m, 1000 s for the layer at y = 0.27 m, 1500 s for the layer at y = 0.40 m, and 2000 s for the layer at y = 0.54 m) and when the grain temperature started to stabilize (after 1250 s for the layer at y = 0.15 m, 2000 s for the layer at y = 0.27 m, 2750 s for the layer at y = 0.40 m and 3550 s for the layer at y = 0.54 m), the analytical solution, elaborated in this paper, was in good agreement with the experimental data.

6.2. Numerical verification

For each approximation used, the results regarding discretisation errors and effective orders for the temperature T, at y = 0.15 m and t = 450 s, are presented. In the tests, the representative mesh size, h, was calculated as $h = \Delta y = \frac{\Delta t}{2}$, with $t_f = 1600$ s.

The behaviours of the discretisation errors with mesh refinement, for all methods used, can be seen in Fig. 5. It can be seen that the discretisation error decreased following the refinement of the mesh for all methods under study. Furthermore, the slopes of the curves of the first-order methods (UDS - Explicit, UDS - Implicit, UDS - Crank-Nicolson, CDS - Implicit, UDS-C - Implicit and UDS-C - Crank-Nicolson) were approximately equal, indicating that the errors tend to decay under the same rates.

It is possible to see the difference in slope between the curves of the first-order approximations and the curves of the second-order approximations (CDS - Crank-Nicolson, RWS, and LS), indicating that the second-order methods performed better, as expected.

Figure 6 shows the effective orders with mesh refinement for all the methods under study.

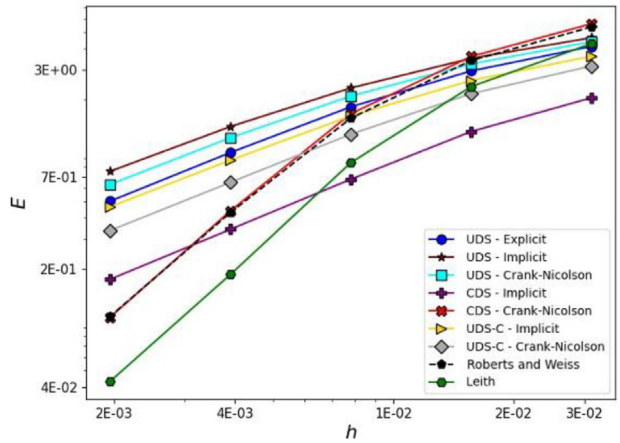

Fig. 5 – Decay of the discretisation errors with mesh refinement for all methods used.

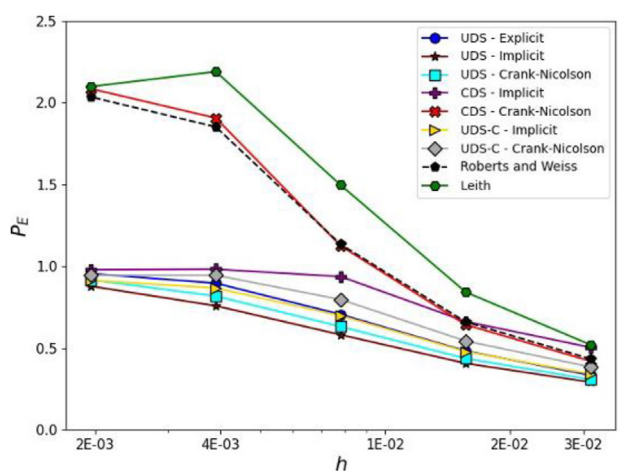

Fig. 6 – Behaviour of the effective orders of discretisation errors with mesh refinement for all methods under study.

In Fig. 6, with the mesh refinement, the effective orders (p_E) of each method can be seen to converge to their asymptotic orders (p_L) shown in Table 1, corroborating their results.

6.3. *Numerical results*

In order to compare the methods used, Table 2 shows the L_2 - norms for the heights of y = 0.15 m, y = 0.27 m, y = 0.40 m and y = 0.54 m, for all methods with respect to the number of unknowns ($N = N_y N_t$) used.

As presented in Table 2 the L_2 - norms decreased with the increase in the number of unknowns for all methods.

Figure 7 shows the data from Table 2 in a graph L_2 *versus* the number of unknowns for all the methods used.

As observed in Fig. 7, the slopes of the curves of the second-order methods were greater than the slopes of the curves of the first-order methods. Thus, with the increase in the number of unknowns, the L_2 - norms obtained by the second-order methods were considerably smaller than the L_2 - norms obtained by the first-order methods.

It is possible to verify in Table 2 and Fig. 7 that the methods with the lowest L_2 - norms in relation to the analytical solution were: UDS - Explicit, CDS - Crank-Nicolson, RWS, and LS.

For the largest number of unknowns tested (N = 131,072), the difference between the UDS - Explicit method (best first-order method) and the CDS - Crank-Nicolson, RWS, and LS

Table 3 – CPU time (s) of the methods used in relation to the number of unknowns.

N	UDS - Explicit	CDS - Crank-Nicolson	RWS	LS
2048	0.8732E-03	0.9179E-03	0.9120E-03	0.9646E-03
8192	0.3477E+00	0.3593E+00	0.3576E+00	0.3632E+00
32,768	0.1372E+01	0.1407E+01	0.1415E+01	0.1427E+01
131,072	0.5484E+01	0.5594E+01	0.5603E+01	0.5685E+01
524,288	0.2193E+02	0.2218E+02	0.2224E+02	0.2248E+02

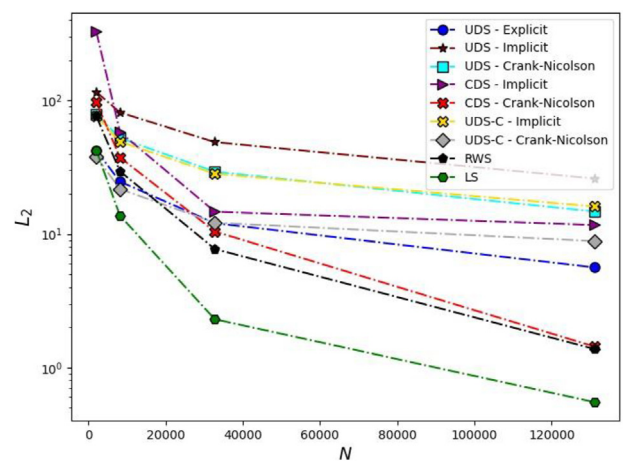

Fig. 7 – L_2 - norm *versus* the number of unknowns.

Table 2 – L_2 - norms with respect to the number of unknowns for each method used.

N	2048	8192	32,768	131,072
UDS - Explicit	0.4239E+02	0.2468E+02	0.1205E+02	0.5625E+01
UDS - Implicit	0.1159E+03	0.8132E+02	0.4885E+02	0.2603E+02
UDS - Crank-Nicolson	0.7888E+02	0.5240E+02	0.2929E+02	0.1472E+02
CDS - Implicit	0.3297E+03	0.5804E+02	0.1468E+02	0.1167E+02
CDS - Crank-Nicolson	0.9746E+02	0.3749E+02	0.1044E+02	0.1434E+01
UDS-C - Implicit	0.7666E+02	0.4920E+02	0.2828E+02	0.1607E+02
UDS-C - Crank-Nicolson	0.3793E+02	0.2173E+02	0.1214E+02	0.8846E+01
RWS	0.7648E+02	0.2950E+02	0.7728E+01	0.1375E+01
LS	0.4248E+02	0.1372E+02	0.2297E+01	0.5508E+00

methods were 4.19138 °C, 4.24993 °C, and 5.074943 °C, respectively; which shows that the second-order methods had considerably better results than the best first-order method.

Table 3 summarizes the CPU times obtained by the methods that showed the best performances (UDS - Explicit, CDS - Crank-Nicolson, RWS, and LS) for different values of $N = N_y N_t$.

As the number of unknowns increased, the CPU time also increased for all methods, and even though the CPU time increased for all methods, there was no significant difference between them.

It is possible to observe that the UDS - Explicit method had a lower CPU time than the other methods, but with a maximum difference of 0.24972, 0.30511, and 0.54912 s, for CDS - Crank-Nicolson, RWS, and LS, respectively.

Given the substantial differences in the L_2 -norms, shown in Table 2 and Fig. 7, and the minor difference in CPU times, the CDS - Crank-Nicolson, RWS, and LS methods proved to be better than the UDS - Explicit method, widely used in the literature (Lopes et al., 2006, 2014, 2015; Thorpe, 2001b); especially LS method (see Fig. 7).

Therefore, the LS method, not yet explored in the literature, is recommended to numerically solve the Thorpe model.

7. Conclusions

This paper proposed an analytical solution using the MMS, based on experimental data, for the mathematical model developed by Thorpe for the grain mass aeration problem. The FDM was applied, and the behaviours of several types of numerical approximations that had not yet been explored in the literature for this problem were investigated. For the second-order methods, artificial viscosity was inserted to avoid non-physical oscillations of the problem. Smaller errors were obtained using the CDS - Crank-Nicolson, RWS, and LS methods, in contrast to the widely used method, the UDS - Explicit. Moreover, the difference in CPU time between the methods studied and the one widely used in the literature was minimal. In light of the above, the LS method is recommended to numerically solve the problem of grain mass aeration proposed by the Thorpe model.

Declaration of Competing Interest

The authors declare that they have no known competing financial interests or personal relationships that could have appeared to influence the work reported in this paper.

Acknowledgments

This work was supported in part by the Coordenação de Aperfeiçoamento de Pessoal de Nível Superior - Brasil (CAPES) - Finance Code 001.

REFERENCES

Antunes, A. M., Devilla, I. A., Neto, A. C., Alves, B. G., Alves, G. R., & Santos, M. M. (2016). Development of an automated system of aeration for grain storage. *African Journal of Agricultural Research, 11*(43), 4293–4303. https://doi.org/10.5897/AJAR2016.11538

Brooker, D. B., Bakker-Arkema, F. W., & Hall, C. W. (1992). *Drying and storage of grains and oilseeds*. Springer Science & Business Media.

Campbell, J., & Vignjevic, R. (2009). Artificial viscosity methods for modelling shock wave propagation. In *Predictive modelling of dynamic processes* (pp. 349–365). Boston, MA: Springer. https://doi.org/10.1007/978-1-4419-0727-1_19.

Campbell, L. J., & Yin, B. (2007). On the stability of alternating-direction explicit methods for advection-diffusion equations. *Numerical Methods for Partial Differential Equations: An International Journal, 23*(6), 1429–1444. https://doi.org/10.1002/num.20233

Chung, D. S., & Pfost, H. B. (1967). Adsorption and desorption of water vapor by cereal grains and their products Part I: Heat and free energy changes of adsorption and desorption. *Transactions of the ASAE, 10*(4), 549–551. https://doi.org/10.13031/2013.39726

Daum, T. (2019). ICT applications in agriculture. In *, 1. Encyclopaedia of Food Security and Sustainability* (pp. 255–260). https://doi.org/10.1016/B978-0-08-100596-5.22591-2

Dehghan, M. (2005). Quasi-implicit and two-level explicit finite-difference procedures for solving the one-dimensional advection equation. *Applied Mathematics and Computation, 167*(1), 46–67. https://doi.org/10.1016/j.amc.2004.06.067

Fleurat-Lessard, F. (2002). Qualitative reasoning and integrated management of the quality of stored grain: A promising new approach. *Journal of Stored Products Research, 38*(3), 191–218. https://doi.org/10.1016/S0022-474X(01)00022-4

Hunter, A. J. (1987). An isostere equation for some common seeds. *Journal of Agricultural Engineering Research, 37*(3–4), 93–105. https://doi.org/10.1016/S0021-8634(87)80008-2

Jayas, D. S., & Cenkowski, S. (2006). Grain property values and their measurement. In *Handbook of industrial drying*. CRC Press. https://doi.org/10.1201/9781420017618.

Jia, C., Sun, D. W., & Cao, C. (2001). Computer simulation of temperature changes in a wheat storage bin. *Journal of Stored Products Research, 37*(2), 165–177. https://doi.org/10.1016/S0022-474X(00)00017-5

Khatchatourian, O. A., & Oliveira, F. A. (2006). Mathematical modelling of airflow and thermal state in large aerated grain storage. *Biosystems Engineering, 95*(2), 159–169. https://doi.org/10.1016/j.biosystemseng.2006.05.009

Lax, P., & Wendroff, B. (1960). Systems of conservation laws. *Communications on Pure and Applied Mathematics, 13*(2), 217–237. https://doi.org/10.1002/cpa.3160130205

Leith, C. E. (1965). Numerical simulation of the earth's atmosphere. *Methods in Computational Physics, 4*(1), 1–28.

Lopes, D. C., Martins, J. H., Melo, E. C., & Monteiro, P. M. B. (2006). Aeration simulation of stored grain under variable air ambient conditions. *Postharvest Biology and Technology, 42*(1), 115–120. https://doi.org/10.1016/j.postharvbio.2006.05.007

Lopes, D. C., Neto, A. J. S., & Júnior, R. V. (2015). Comparison of equilibrium models for grain aeration. *Journal of Stored Products Research, 60*, 11–18. https://doi.org/10.1016/j.jspr.2014.11.001

Lopes, D. C., Neto, A. J. S., & Santiago, J. K. (2014). Comparison of equilibrium and logarithmic models for grain drying. *Biosystems Engineering, 118*, 105–114. https://doi.org/10.1016/j.biosystemseng.2013.11.011

Marchi, C. H., Martins, M. A., Novak, L. A., Araki, L. K., Pinto, M. A. V., Gonçalves, S. F. T., Moro, D. F., & Freitas, I. S. (2016). Polynomial interpolation with repeated Richardson extrapolation to reduce discretization error in CFD. *Applied Mathematical Modelling, 40*(21–22), 8872–8885. https://doi.org/10.1016/j.apm.2016.05.029

Melland, P., Albright, J., & Urban, N. M. (2021). Differentiable programming for online training of a neural artificial viscosity function within a staggered grid Lagrangian hydrodynamics scheme. *Machine Learning: Science and Technology, 2*(2), Article 025015. https://doi.org/10.1088/2632-2153/abd644

Mousa, M. M., & Ma, W. X. (2020). Efficient modelling of shallow water equations using method of lines and artificial viscosity. *Modern Physics Letters B, 34*(4), Article 2050051. https://doi.org/10.1142/S0217984920500517

Navarro, S., & Noyes, R. T. (2001). *The mechanics and physics of modern grain aeration management*. CRC Press.

Nuttall, J. G., O'leary, G. J., Panozzo, J. F., Walker, C. K., Barlow, K. M., & Fitzgerald, G. J. (2017). Models of grain quality in wheat - a review. *Field Crops Research, 202*, 136–145. https://doi.org/10.1016/j.fcr.2015.12.011

Nyarko, D. A., & Kozári, J. (2021). Information and communication technologies (ICTs) usage among agricultural extension officers and its impact on extension delivery in Ghana. *Journal of the Saudi Society of Agricultural Sciences, 20*(3), 164–172. https://doi.org/10.1016/j.jssas.2021.01.002

Oberkampf, W. L., & Blottner, F. G. (1998). Issues in computational fluid dynamics code verification and validation. *AIAA Journal, 36*(5), 687–695. https://doi.org/10.2514/2.456

Oliveira, F., Khatchatourian, O. A., & Bilhain, A. (2007). Thermal state of stored products in storage bins with aeration system: Experimental-theoretical study. *Engenharia Agrícola, 27*(1), 247–258.

Oliveira, M. L., Pinto, M. A. V., Gonçalves, S. F. T., & Rutz, G. V. (2018). On the robustness of the xy-Zebra-Gauss-Seidel Smoother on an anisotropic diffusion problem. *Computer Modeling in Engineering and Sciences, 117*(2), 251–270.

Pfost, H. B., Rengifo, G. E., & Sauer, D. B. (1976). High temperature, high humidity grain storage. *Transactions of the ASAE, 76*. St. Joseph, MI.

Rigoni, D., & Kwiatkowski Jr., J. E. (2020). Using the multigrid method to improve the performance of aeration process simulation. *Proceeding Series of the Brazilian Society of Computational and Applied Mathematics, 7*, 010331-1–010331-2.

Roache, P. J. (1998). *Fundamentals of computational fluid dynamics*. Hermosa Publishers.

Roberts, K. V., & Weiss, N. O. (1966). Convective difference schemes. *Mathematics of Computation, 20*(94), 272–299. https://doi.org/10.2307/2003507

Roy, C. J. (2005). Review of code and solution verification procedures for computational simulation. *Journal of Computational Physics, 205*(1), 131–156. https://doi.org/10.1016/j.jcp.2004.10.036

Sinicio, R., Muir, W. E., & Jayas, D. S. (1997). Sensitivity analysis of a mathematical model to simulate aeration of wheat stored in Brazil. *Postharvest Biology and Technology, 11*(2), 107–122. https://doi.org/10.1016/S0925-5214(97)00017-3

Tannehill, J. C., Anderson, D. A., & Pletcher, R. H. (1997). *Computational fluid mechanics and heat transfer* (Vol. 2). Taylor & Francis.

Thomas, L. (1949). *Elliptic problems in linear differential equations over a network: Watson Scientific Computing Laboratory*. New York: Columbia University.

Thompson, T. L. (1972). Temporary storage of high-moisture shelled corn using continuous aeration. *Transactions of the ASAE, 15*(2), 333–337. https://doi.org/10.13031/2013.37900

Thompson, T. L., Peart, R. M., & Foster, G. H. (1968). Mathematical simulation of corn drying a new model. *Transaction of the ASAE, 11*(4), 582–586.

Thorpe, G. R. (2001a). Ambient air properties in aeration. In *The mechanics and physics of modern grain aeration management* (pp. 79–120). CRC Press.

Thorpe, G. R. (2001b). Physical basic of aeration. In *The mechanics and physics of modern grain aeration management* (pp. 125–185). CRC Press.

Van Genuchten, M. T., & Alves, W. J. (1982). *Analytical solutions of the one-dimensional convective-dispersive solute transport equation*. United States Department of Agriculture, Economic Research Service.

Von Neumann, J., & Richtmyer, R. D. (1950). A method for the numerical calculation of hydrodynamic shocks. *Journal of Applied Physics, 21*(3), 232–237. https://doi.org/10.1063/1.1699639

Xuan, G., Zheng, H., Xiaoyu, S., & Bin-Sheng, W. (2017). A two-dimensional lattice Boltzmann method for compressible flows. *Acta Informatica Malaysia (AIM), 1*(1), 32–35. https://doi.org/10.26480/aim.01.2017.32.35

Ziegler, V., Paraginski, R. T., & Ferreira, C. D. (2021). Grain storage systems and effects of moisture, temperature and time on grain quality-A review. *Journal of Stored Products Research, 91*, Article 101770. https://doi.org/10.1016/j.jspr.2021.101770